DIRICT TORQUE CONTROL OF PM SYNCHRONOUS MOTOR

Gamal M. A. Sarhan*, Abd El-Nasser A. Nafeh*, Mohamed H. Shalan*
* High Institute of Technology, Benha University, El-Qalubia, Egypt
E-mails: abdelnassern@yahoo.com, mohamed.shaalan@bhit.bu.edu.eg

***Abstract*- In recent years the industrial application areas of the high performance AC drives based on Direct Torque Controller (DTC) technique have gradually increased due to its advantages over the field oriented control technique. Direct torque control (DTC) is one of the most excellent control strategies of torque control in PMSM. It is considered as an alternative to the field oriented control (FOC) or vector control technique. These two control strategies are different on the operation principle but their objectives are the same. They aim to control effectively the torque and flux. Torque control of an PMSM based on DTC strategy has been developed and a comprehensive study is presented in this research. The performance of this control method has been demonstrated by simulations performed using a versatile simulation package, Matlab/Simulink. Several numerical simulations have been carried out in a steady state and transient operation on a speed control mode. Implementation of an actual drive system based on the suggested DTC including software and hardware, to validate its performance practically is presented. The suggested control strategy guarantees very good dynamic and steady state characteristics. The practical and simulation results show that the used DTC gives good dynamic performance and good tracking response.**

Keywords – Direct Torque Controller, Permanent Magnet Synchronous Motor, Vector control, Matlab/Simulink.

I. INTRODUCTION

A significant technological change has occurred in motor drive system in recent years. The main feature of the drive system refers to its capability to operate within the given speed and torque limits. Other desirable features of variable speed, drives include low space requirement, low maintenance, and capability of the speed or torque to follow the speed or torque command. Increasing interest has been shown in using permanent magnet synchronous motors with variable-frequency inverters in adjustable-speed. Drive, taking advantage of increased efficiency and power factor product to reduce volt-ampere requirement [1,2,3].

The basic DTC scheme is indicated in Fig.1; torque and flux signals are obtained from the estimator. These are regulated by using two hysteresis controllers. The hysteresis controller outputs in turn switch the three inverter legs, applying a set of voltage vectors across the motor. Although the switching table- based DTC (basic DTC) has many advantages over vector control, one of its major drawbacks is the high torque and flux ripples. The switching frequency is also not constant, varying with speed, load torque, and the hysteresis bands selected. The inverter keeps the same state until the outputs of the hysteresis controllers change their outputs at the sampling point. Hence, the DTC scheme generates a discrete switching function, i.e., the pulse width of inverter must be the multiple of the sampling interval. It may be noted that the hysteresis controllers were also used in current-regulated PWM inverters, however, due to their varying switching frequency, new schemes such as the proportional–integral (PI) PWM controller and space-vector-based regulator.

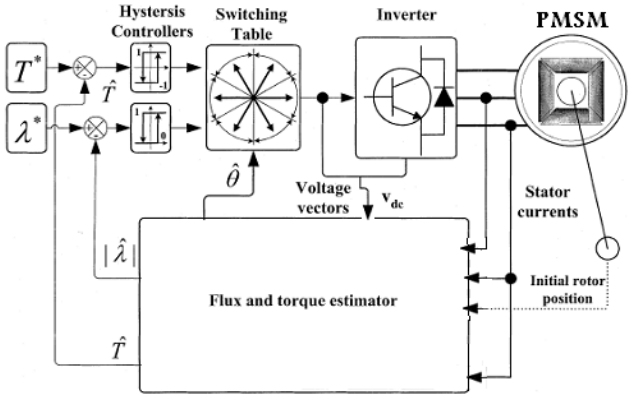

Fig.1 System diagram of a typical DTC PMSM drive system.

DTC strategy give a fast and good dynamic performance and can be considered as an alternative to the FOC strategy therefore, in recent years the industrial application areas of the high performance AC drives based on DTC technique have gradually increased due to the following advantages over the field oriented control technique, such as: (i) Excellent dynamic performance. (ii) Precise and quick control of stator flux and electromagnetic torque. (iii) Absence of coordinate transformation, which reduce the complexity of algorithms involved in FOC. (iv) Robust against machine parameters variations. (v) No current control loops. A DTC Drive system, which is based on a pre-fixed hysteresis bands for both torque and flux controllers, suffers from a varying switching frequency, which is a function of a motor speed, stator/ rotor fluxes, and stator voltage; it is also not constant in steady state. At low speed, an appreciable level of acoustic noise is present, which is mainly due to the low inverter switching frequency. The high frequency is limited by the switching characteristics of the power devices. Therefore, there will be large torque ripples and distorted waveforms in currents and fluxes. Thus there will be a varying device switching frequency. Variable switching frequency is undesirable and is limited by the thermal condition of the switching devices and maximum switching frequency of the devices. Therefore, there will be a large torque ripples and distorted waveforms in currents and fluxes.

Several solutions have been proposed to keep constant switching frequency [4].

PMSM have the following advantages over DC motors:
Less audible noise, longer life, spark-less (no fire hazard), higher speed, higher power density and smaller size, and better heat transfer. Also, *PMSM have the following advantages over IMs:*
Higher efficiency, higher power factor, higher power density for lower than 10kW applications, resulting in smaller size, better heat transfer

The above comparison shows that the PMSM and BDCM are superior to the induction motor for low power applications. The operation of the BDCM and the PMSM is very similar from a fundamental point of view. Therefore, all the analysis and control strategies developed for the PMSM readily applies to the BDCM [5].

PMSMs can offer significant efficiency advantages over induction machines when employed in adjustable-speed drives. The PM motor operates at synchronous speed and therefore does not have the slip losses inherent in induction motor operation. In addition, since much of the excitation in the PM motor is provided by the magnets, the PM motor will have smaller losses associated with the magnetizing component of stator current, These factors make the PM motor an attractive alternative to the induction machine in drives where overall efficiency is critical, notably in pump, compressor, or fan drives [6,7,8,9,10].

II. *Dynamic Model of PMSM in (αβ) Frame*

The PMSM is the same as the field excited synchronous motor from the analytical point of view. The only exception is that the rotor field due to permanent magnet excitation gives a constant flux.

The model of PMSM without damper winding has been developed on rotor reference frame using the following assumptions:
1) Saturation is neglected.
2) The induced EMF is sinusoidal.
3) Eddy currents and hysteresis losses are negligible.
4) There are no field current dynamics.

The system considered is a permanent magnet synchronous motor having permanent magnets mounted on the rotor, and a sinusoidal flux distribution. A dynamic model for this motor in a stator-fixed reference frame (α β), by choosing the current components iα, iβ the rotor speed ωr ,and the rotor position θr as state variables is as Follows:

$$\frac{d}{dt}i\alpha = -\frac{Rs}{Ls}\,i\alpha + \frac{\lambda f}{Ls}\,\omega r \sin(\theta r) + \frac{V\alpha}{Ls} \quad (1)$$

$$\frac{d}{dt}i\beta = -\frac{Rs}{Ls}\,i\beta - \frac{\lambda f}{Ls}\,\omega r \cos(\theta r) + \frac{V\beta}{Ls} \quad (2)$$

$$\frac{d}{dt}\omega r = \frac{3}{2}\frac{\lambda f}{Jm}\,(i\beta\cos(\theta r) - i\alpha\sin(\theta r)) - \frac{Bm}{Jm}\omega r - \frac{TL}{J} \quad (3)$$

$$\frac{d}{dt}\theta r = \omega r \quad (4)$$

$$Te = \frac{3}{2}\,\lambda f\,(i\beta\cos(\theta r) - i\alpha\sin(\theta r)) \quad (5)$$

Where,
Rs stator per-phase resistance
Ls stator per-phase inductance
λf permanent magnet flux linkage
Jm rotor moment of inertia
Bm viscous damping.

The voltage components,Vβ, and the average load torque TL are the deterministic control inputs of the system. Both the voltage and current components are measurable quantities. They are obtained from the three phase stator components by a linear transformation:

$$i\alpha = \frac{2}{3}\left(ia - \frac{ib}{2} - \frac{ic}{2}\right) \quad (6)$$

$$i\beta = \frac{(ib - ic)}{\sqrt{3}} \quad (7)$$

Similar equations hold for the voltages.

To summarize, the system is driven by the stator voltages Vα , Vβ , and the resulting outputs are the stator currents iα and iβ. The state space model (1) - (5) is nonlinear due to the cross product of the state variables ωr, iα , iβ and θr [14,15]. The motor parameters used are listed in the Appendix.

III. APPLICATIONS OF DTC FOR PMSM

Direct Torque and Flux Control (DTFC), also termed Direct Torque Control (DTC), has been developed by German and Japanese researchers for use in torque control of high power servo drives. Recently, it has provided an industrial alternative to the field oriented control strategy. DTC is a control philosophy exploiting the torque and flux producing capabilities of ac machines when fed by a simple voltage source inverter that does not require current regulation loops, still attaining similar performance to that obtained from a vector control drive [4,16,17,18].

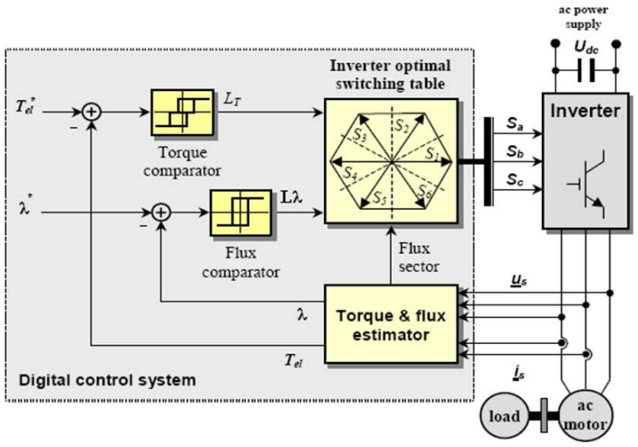

Fig. 2 Basic direct torque control scheme for ac motor drives.

Three control techniques have been employed for implementing DTFC drives: The Switching Table (ST), the Direct Self Control (DSC) and the Direct Vector Modulation Control (DVMC). ST and DSC regulators are of the hysteresis (discrete) type, whereas the DVMC uses digitally

implemented analog controllers such as the PI controllers. The basic DTC scheme for ac motor drives is shown in Fig. 2. The main blocks are the stator flux and electromagnetic torque estimator and the switching vector look-up table [17,19].

For implementing the control loop, the actual stator flux (amplitude and orientation) and electromagnetic torque are calculated by an estimator from the stator voltages and currents in a similar fashion to the reconstruction approach of the direct vector control philosophies (DFOC).

Thus, the flux magnitude strongly depends on the stator voltage. As the stator voltage changes, the stator flux follows rapidly whereas the rotor flux (rotor current) changes are slower and less pronounced than that of the stator flux. This effect modifies the angle between stator and rotor fluxes and consequently the torque increases or decreases. Thus, stator flux and developed torque can be directly controlled by proper selection of the stator voltage, that is selection of consecutive inverter states without coordinate transformations like the ones performed by vector control strategies. The developed torque is obtained by the product of stator current and flux.

In most DTC control schemes, the torque is compared in a three-level hysteresis controller defining the error torque state LT in modulus and sign. The stator flux is compared to its reference value and is fed into a two-level hysteresis controller defining the error flux state Lλ. With this information, a voltage selector determines the stator voltage that is required to increase or decrease the variables (torque or flux) according to the demands. More advanced look-up tables, overcoming DTC related problems as demagnetization at low motor speed, are described in literature, e.g. [17].

IV. CONTROL STRUCTURE

The basic idea of DTC is when the torque is wanted to be increased, a voltage vector which increases the angle between the air gap flux linkage and the stator flux linkage is selected, and vice versa. A block diagram of a DTC system for an ac motor is shown in Fig.2. Two independent hysteresis (bang-bang) controllers control the motor torque and stator flux [16,20,21,22,23]. Therefore, the selection of hysteresis band control range will affect on the performance of the drive system [24]. The inverter switching patterns are generally directly as a function of both the torque error and the flux error. By using only current and voltage measurements, it is possible to estimate the instantaneous stator flux and output torque. The PMSM model is then used to predict the voltage required to drive the flux and torque to the demanded values within a fixed time period.

The stator flux vector λ is obtained by integrating the motor EMF space vector, measured stator currents and stator resistance.

$$\lambda = \int (Vs - RsIs)dt \qquad (8)$$

The stator voltage space vector is calculated using the dc-link voltage Vdc and the gating signals (Sa, Sb, Sc) instead of direct measuring with Hall effect voltage sensors.

$$Vs = 2/3\ Vdc\ [\ Sa + a\ Sb + a^2\ Sc\ ] \qquad (9)$$

Where, $a = e^{j\frac{2\pi}{3}}$

The stator current space vector is calculated from measured stator currents.

$$Is = 2/3\ [\ ia + a\ ib + a^2\ ic\ ] \qquad (10)$$

The motor torque is estimated from Equation (5). Then from Fig.2 the inputs to the switching table block are the torque and flux error, and the stator flux angle information are used to select the suitable switching pattern. Many voltage selection strategies can be utilized as widely discussed in Refs. [16,25,26,27,28,29]. Each strategy affects the drive performance in terms of torque and current ripple, switching frequency, and torque response [21,23,24].

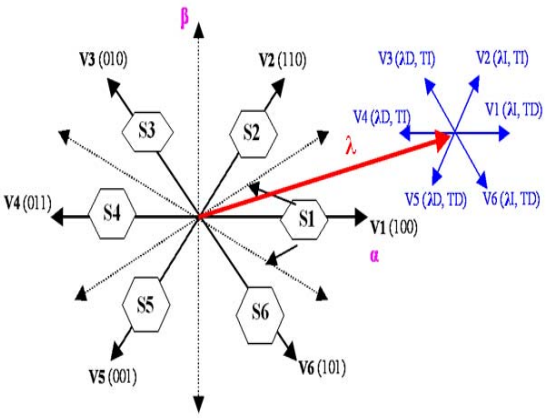

Fig.3 Stator flux vector locus and different possible switching voltage vector lies in sector 1.
λ = Flux, T = Torque, D = Decrease, and I = Increase.

From Fig.3 in order to increase the stator flux magnitude, it is necessary to select the voltage vector, that determines a high radial component along the direction of the stator flux vector λ. On the other hand, if it is needed to increase the torque, it is necessary to select the voltage vector, that determines the highest tangential component along the direction of stator flux vector λ [21,22,23]. The selection table proposed by Takahashi [22] is used as shown in Table (1).

The sectors of the stator flux space vector are denoted from S1 to S6. The hysteresis controller for flux can take two different values, while the torque hysteresis controller can take three different values. The zero voltage vectors V_O and V_7 are selected when the torque error is within the given hysteresis limits i.e. (in case of no change).

Table (1) Optimum selection table for DTC.

L_λ	L_T	S_1	S_2	S_3	S_4	S_5	S_6
1	1	V_2	V_3	V_4	V_5	V_6	V_1
1	0	V_7	V_0	V_7	V_0	V_7	V_0
1	-1	V_6	V_1	V_2	V_3	V_4	V_5
0	1	V_3	V_4	V_5	V_6	V_1	V_2
0	0	V_0	V_7	V_0	V_7	V_0	V_7
0	-1	V_5	V_6	V_1	V_2	V_3	V_4

V. SIMULATION AND ANALYSIS OF RESULTS

The nonlinear mathematical models of PMSM developed before can now be implemented together using the SIMULINK programming language for proper solution to the machine variables such as stator and rotor currents and/or fluxes, electromagnetic torque, and rotor speed under any operating condition with any type of drive controller. The approach is to represent each term of the developed non-linear differential equation by an analogue block. All terms representing the drive system are then connected together in an analogue form to establish the complete SIMULINK analogue model of the drive system. This model can be easily compiled, and digitally simulated in order to produce the solution results that describe the behavior of the motor under any electrical or/and mechanical input disturbances. It must be understood that despite the model of the motor is represented schematically by SIMULINK in an analogue form, the solution is carried out in the compiler digitally using one of the available numerical techniques in the SIMULINK program. Typical numerical solution may be based on Runge-Kutta, Euler, Adams, and other well-known numerical technique [16,30,31,32,33].

First of all, in order to model suggested DTC systems using the SIMULINK, the complete mathematical models of the constituent subsystems must be available. Then, linking the different constructed models together can easily form the complete SIMULINK model of the classical DTC systems. These developed SIMULINK programs include performance and analysis programs of the classical DTC drive motor at different hysteresis bands of flux - different switching frequency and/or torque under any operating disturbance.

Full information of the examined motor and the relevant parameters are given in Appendix. The strategy and the basis of the above-developed programs are the same except the type of the controller used and the type of disturbance imposed on the system. The mathematical model of each considered subsystem is used here to form the SIMULINK model for each subsystem. The complete dynamic models of the direct torque control of PMSM drive systems is shown in Fig.4.

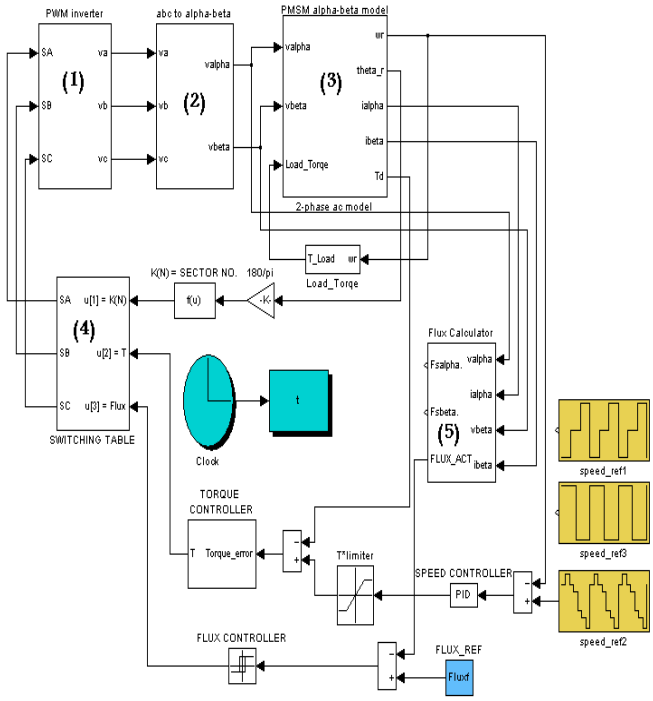

Fig.4 Complete Simulink model of DTC of PMSM drive system.

Based on the modeling and solution approach, the closed loop speed tracking scheme was simulated under variable operating conditions and adopted to enhance the electrodynamics performances of the drive motor. The DTC results are taken at a torque and flux hysteresis bands of 1 % for both. The closed loop DTC model with full load using the parameters in appendix but the simulation results show the stator resistance variation effects cancelation with DTC when variation parameters (Rs , Ls). In particular, the stator time constant of the motor (τ s = Ls / Rs) varies with the temperature and the degree of the magnetic saturation (Ls changes by 20% and Rs changes by 100%). The saturation of the machine increases the field component of the stator current while decreasing the torque component. This effect the peak torque capability of the drive and results in an increase in the acceleration and deceleration on times. The effects of this mismatch between controller and motor parameters both for steady state and dynamic conditions .So that the simulated based on the speed trajectory pattern depicted in Fig.5 and 6 confirms a good agreement between the reference speed trajectory assumed for the DTC model and the speed response of the drive motor.

The dynamic response of the motor reference and actual speed from (+ 1 p.u. to - 1 p.u.) are shown in Fig.5. Adjusting the proportional (Kp) and integral (Ki) speed controller parameters respectively, to give the desired best response can control the speed response.

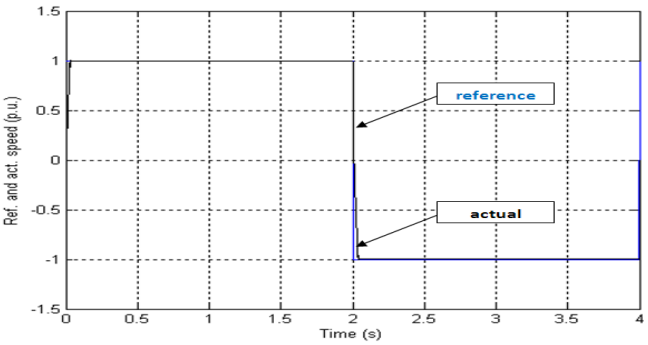

Fig. 5 Dynamic performance of reference and actual speed with full loading.

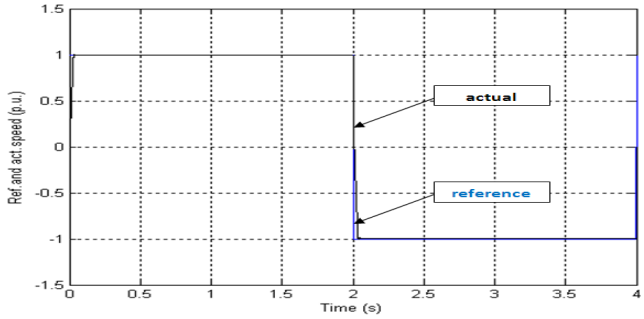

Fig. 6 Dynamic performance of reference and actual speed with full loading and parameters variation.

Figure 7 and 8 indicate the performances of rotor flux due to speed changes. It is noted that the motor flux maintained constant in this speed range while, a distorted and changed flux magnitude especially at the transient instant and at speed reversal with DTC as indicated.

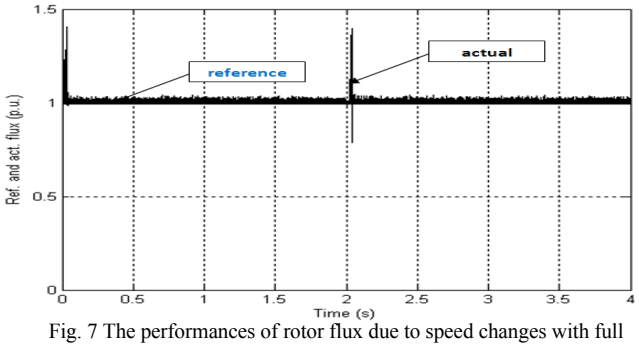

Fig. 7 The performances of rotor flux due to speed changes with full loading.

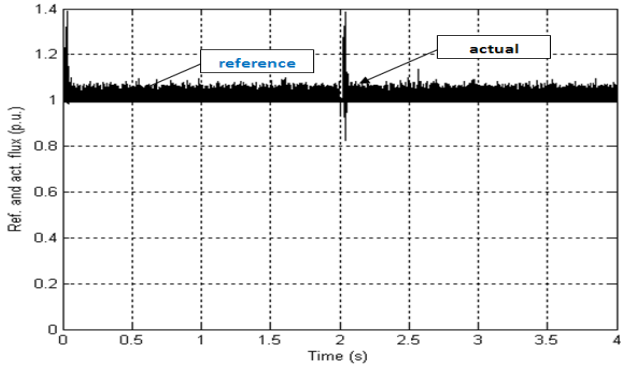

Fig. 8 The performances of rotor flux due to speed changes with full loading and parameters variation.

Figures 9 and 10 show the performances of the motor reference and actual torque corresponding to speed changes in forward and reverse direction as indicated. Also, the reference and actual torque takes their maximum value to provide the accelerating torque at the beginning of the transient instant. The output of speed controller is the reference torque while, the actual torque is the estimated one.

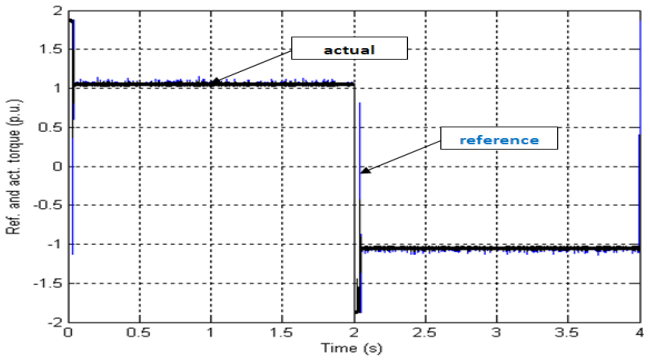

Fig.9 The performances of the motor reference and actual torque corresponding to speed changes with full loading.

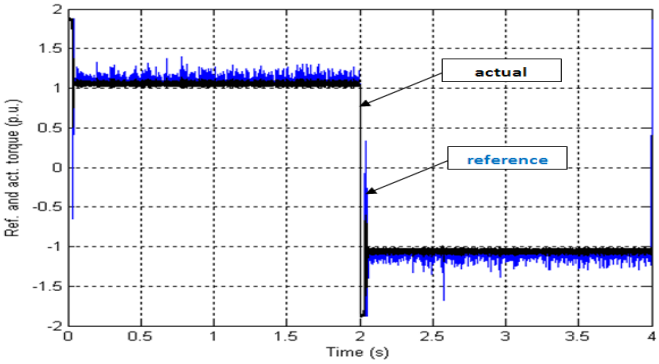

Fig.10 The performances of the motor reference and actual torque corresponding to speed changes with full loading and parameters variation.

Figures 11 and 12 show the two-phase stationary stator fluxes at the transient, steady state, and instant of speed reversing. The fluxes phase sequences are reversed in the instant of speed reversing and maintained at its constant value to keep the V/f ratio constant. Figures 13 and 14 represent the two-phase stationary reference frame currents during starting and steady state. It can be seen that the currents have a phase shift of 90° from each other during starting, steady state, reversed, and back to steady state. As we see, the benefit of the DTC technique is clear here as indicated by the following important issues: Minimum transient response, minimum rise time, minimum overshoot and minimum undershoot, fast response, and zero steady state error. Also, the system has a very good control over the speed tracking application and torque with soft starting operation.

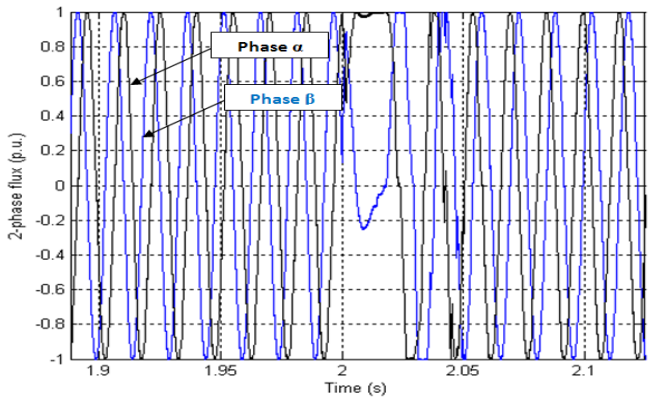

Fig.11 Two-phase stationary stator fluxes due to speed changes with full loading.

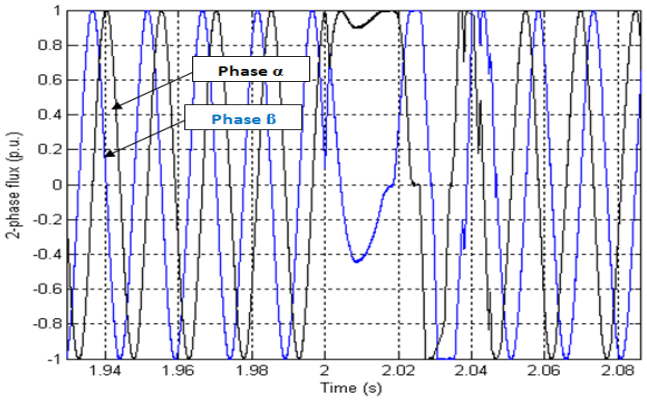

Fig.12 Two-phase stationary stator fluxes due to speed changes with full loading and parameters variation.

Figures 15 and 16 show the flux position angle or the electrical rotor position ramp signal at 4000 rpm where the flux position angle is varying in a linear shape from (0 to 360) degree or from (0 to 6.2832) radian in estimations as indicated. Figure 15 shows the effect of speed reversal on two-phase stationary reference frame flux components and the associated flux position angle. From these figures it is noted that, when the speed is in forward direction of rotation the slope of the flux position is positive. Also, when the speed in backward direction the slope of the flux positions is negative. At the instant of speed reversal, the two-phase stationary reference frame flux components reverses their phase sequences with maintaining their amplitude constants. Consequently, the slope of the flux position is reverse from positive slope to negative slope when speed change from forward to backward direction of rotations and vice versa.

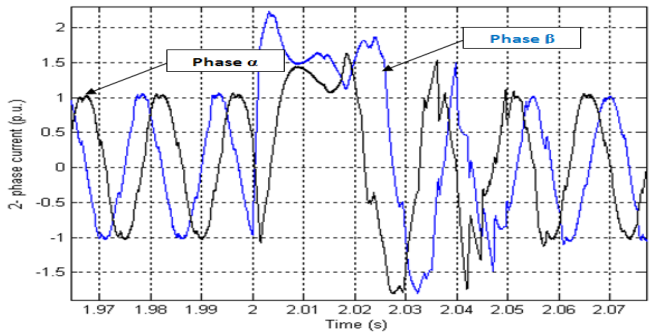

Fig.13 Two-phase stationary reference frame currents due to speed changes with full loading.

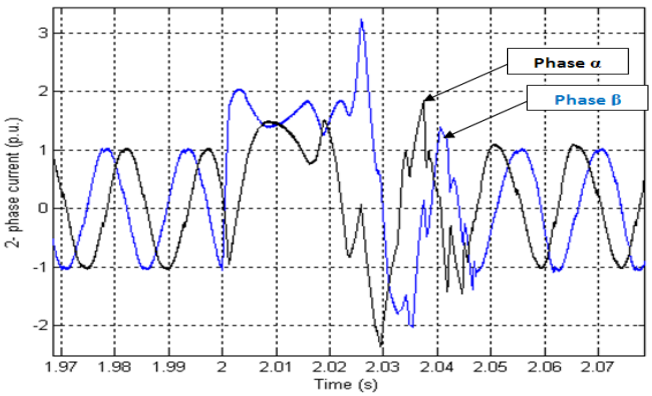

Fig.14 Two-phase stationary reference frame currents due to speed changes with full loading and parameters variation.

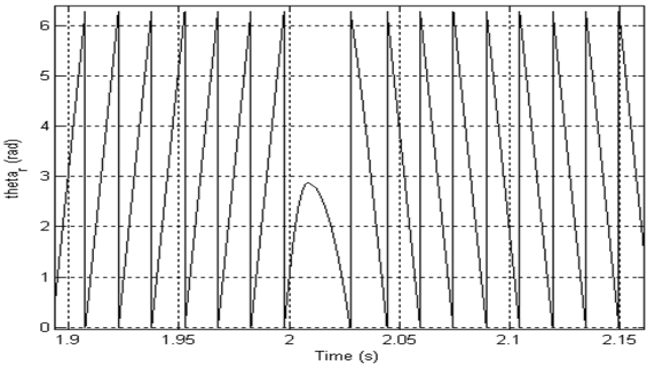

Fig.15 The flux position angle or the electrical rotor position ramp signal at 4000 rpm when speed reversal.

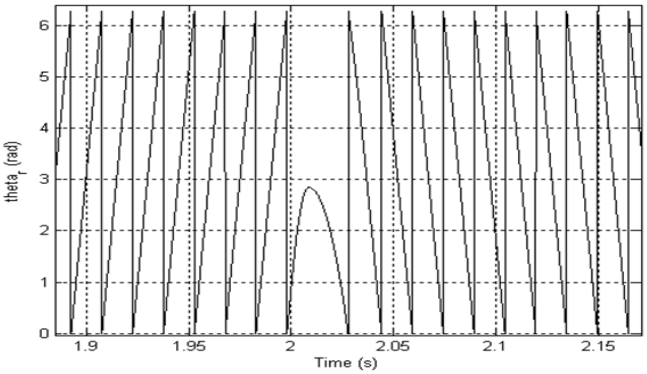

Fig.16 The flux position angle or the electrical rotor position ramp signal at 4000 rpm when speed reversal and parameters variation.

The above simulation results verify the possibility of the suggested control scheme, to be practically implemented. The sets of PI controller parameters tuned to give the best performance. The speed controller parameters are:
KP = 4 and KI = 0.5. These values will be used as the initial values for the parameters of PI controllers in the practical system.

VI. System Implementation

A) The Test Rig of the PMSM Models:

The objective of this item to illustrate the experimental set up of the implemented system to support the theoretical analysis. The experimental work, which is conducted in this paper, is based on, the micro-controller variable speed drive system

running under different conditions. Test results are compared with simulation and the necessary discussions are implemented. The experimental results of this proposed drive system are based mainly on PMS motor and displayed facilities using four-channel digital storage oscilloscope "Tektronix-TDS2014". The results are recorded by snap shots of different examined cases and then analyzed when required.

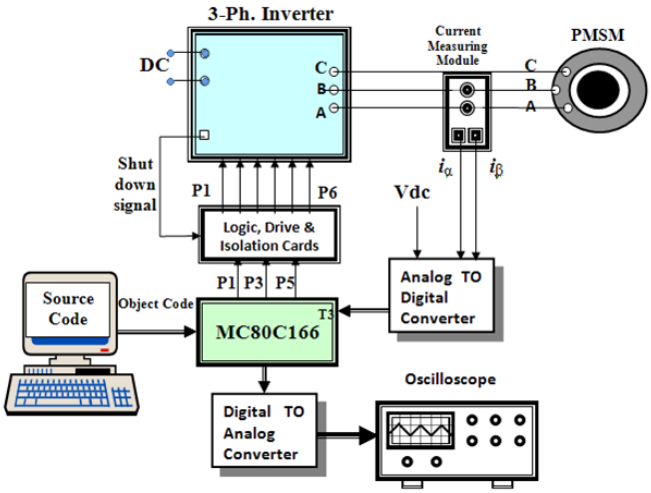

Fig.17 Connection diagram of the implemented DTC system.

Figure 17 represents the schematic connection between the different modules in the complete inverter drive system. The figure indicates that the main elements of the experimental system arranged for this study are:

* The PC with the necessary software and the interfacing developed specially for this investigation.
* The micro-controller, family SAB80C166.
* The data acquisition logic card acting as an interface between the microcontroller and the 3-phase inverter circuits.
* Hall effect current sensors essentially to measure the actual current under any operating condition and then it is used to compute the (α-β) current components in the stationary (α-β) reference frame.
* Hall effect voltage sensor essentially to measure the actual DC-link voltage under any operating condition and then it is used to compute the (α-β) voltage components in the stationary (α-β) reference frame with the aid of the switching states (Sa, Sb, and Sc).
* The examined PMSM, their parameters are given in Appendix.

In the test rig, the developed source code is compiled into an object code and then transmitted from the computer to the micro-controller card through the interface serial port RS232. The proposed program mainly generates the control signals necessary for the controllable gating of the IGBT used in the drive system. These signals are directed to finally to the six IGBT elements of the Inverter Bridge. The main supply to the inverter is dc source produced from a dc generator to prevent the inrush current of autotransformer in case of dynamics. It is seen in the experimental set up figure 17 that only two current lines of the three output lines from the inverter are passed through the Hall effect current measuring module to be measured. These two measured currents are then used to detect the third one hence all of them are used to compute the (α-β) current components in the stationary (α-β) reference frame.

B) The Experimental Results and Discussions:

The dynamic response of the motor with adjusting by trial and error the proportional (Kp) and integral (Ki) speed controller parameters to give the best dynamic response. This section demonstrates the experimental results taken from the DTC drive system such as:

- Performance of motor rotor position.
- Performance of motor currents.

Figure 18 shows the performance of the steady state estimated two-phase direct and quadrature current components corresponding to 500 rpm forward speed and Fig.19 indicates the performance of the flux position or rotor position at 500 rpm forward speed. Also, they have nearly sinusoidal waveforms without any ripples and the flux position angle, is varying in a linear shape from (0 to 360) degree as indicated in figure 19.

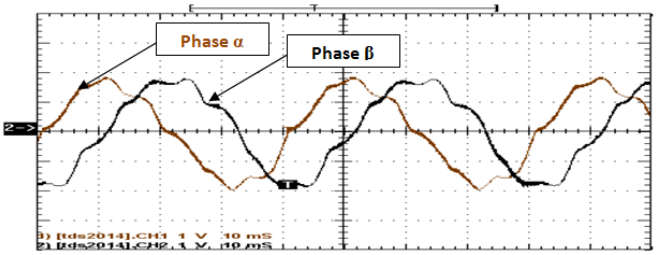

Fig.18 Performance of the steady state estimated two-phase current components corresponding to 500 rpm forward speed.

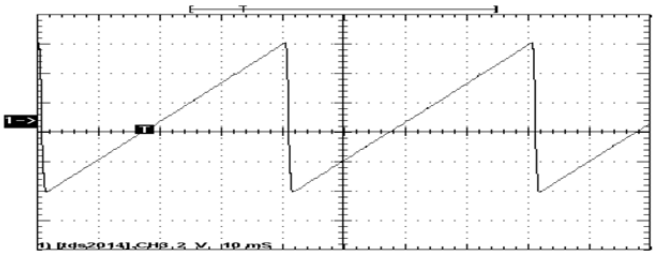

Fig.19 Performance of the rotor position at 500 rpm forward speed.

The performance of the steady state estimated two-phase direct and quadrature current components at 500 rpm at reverse direction are indicated in Fig.20 and the performance of the rotor position at 500 rpm at reverse direction are indicated in Fig.21. It is to be noted that the actual speed track the reference speed and the measured speed is filtered using a low pass filter to make a good accuracy of response in transient and in steady state operation. Also, the fine tuning of the PI speed controller by trial and error is done to make the steady state error equals to zero so that, a good speed response is obtained. Also, the estimated value approximately equals to the reference value.
When the speed is reversed from forward to backward the direct and quadrature current components is reverse their phase sequence with maintaining of their amplitude constants in transient and steady state periods and vice versa to match the new case.

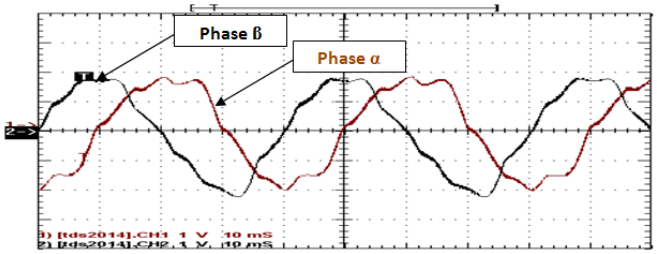

Fig.20 performance of the two-phase current components at 500 rpm at reverse direction.

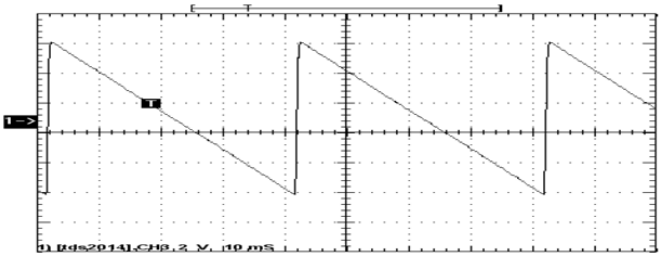
Fig.21 performance of the rotor position at 500 rpm at reverse direction.

When speed is reversed from backward to forward Figs.22, 23, 24 and 25, the drive system gives a very fast and smooth dynamic response. Also, the steady state speed when reversed from forward to backward and vice versa is reached in approximately 250 ms. As indicated from these figures the use of DTC gives a fast and better response in transient and in steady state periods therefore, a good dynamic response is obtained.

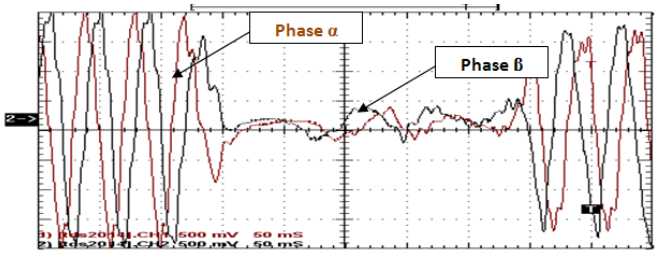

Fig.22 Close view of the two-phase current components when the speed is reversed from forward to backward at 500 rpm.

A little distorted and improved current waveform is obtained by using the direct torque control technique. Increasing the switching frequency reduces the current ripples but this is restricted with the maximum switching frequency of the power transistor, this will case higher switching losses. A compromise between the quality of the output current and the inverter switching losses is the key of the switching frequency choice [16].

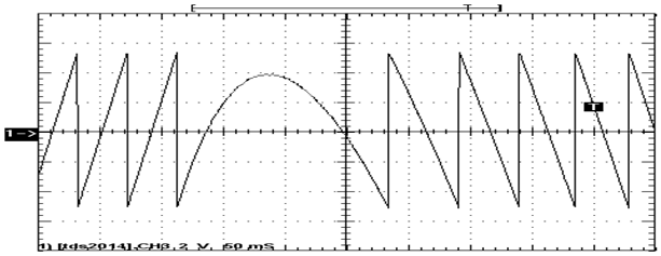
Fig.23 Close view of the rotor position when the speed is reversed from forward to backward at 500 rpm.

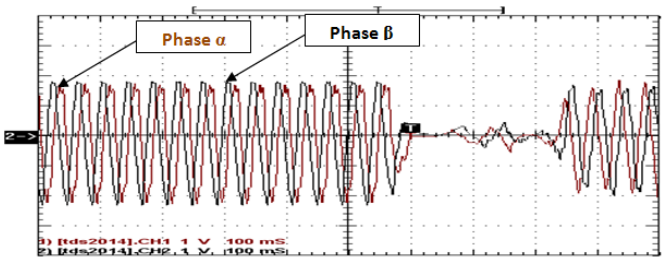

Fig.24 Close view of the two-phase current components when the speed is reversed from backward to forward at 500 rpm.

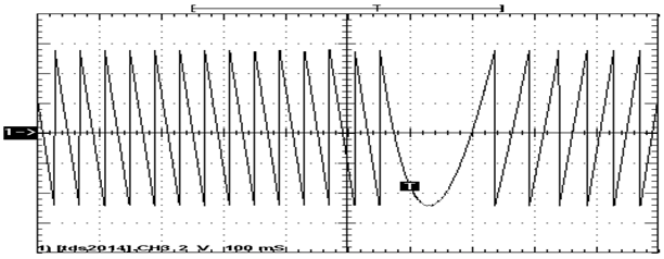
Fig.25 Close view of the rotor position when the speed is reversed from backward to forward at 500 rpm.

Figures 22, 23, 24 and 25 show the effect of speed reversal on direct and quadrature two-phase stationary reference frame current components and the associated flux position angle. From these figures it is noted that when the speed is in backward direction of rotation the slope of the flux position is negative. When speed in forward direction of rotation, the slope of the flux positions is positive and varying from (0 to 360) degree. At the instant of speed reversal, the direct and quadrature two-phase stationary reference frame current components reverses their phase sequence. Consequently, the slope of the flux position is reverse from negative slope to positive slope when speed change from backwards to forward direction of rotations and vice versa. A good performance of currents of the motor are obtained. Also, these two-phase currents are perpendicular to each other i.e. the phase shift between direct and quadrature components are 90 degree electrically and they are nearly sinusoidal waveforms.

VII. CONCLUSION

This paper introduced a developed algorithm based on DTC that successfully operates even in cases of rapidly changing conditions. The complete dynamic model of the DTC system, with hysteresis controller, has been developed and simulated by using MATLAB-SIMULINK. The DTC is designed and selected to give the best transient and steady state response, be simple as possible to make its software implementation easy, and to save memory usage. The MATLAB-SIMULINK models established here proved to be reliable for a better understanding of the fast dynamic performance of the DTC for PMSM drive systems. The study indicates the superiority of the DTC system over the conventional control method. The simulation results confirms that **a** fast and good response of the drive system. A fast and good dynamic response of speed or torque tracking can be achieved by controlling the switching frequency of the PWM.

The experimental set up including the microcontroller and the established interfacing has contributed greatly to obtain some significant experimental results for comparison with the corresponding simulation. Recorded measurements confirms that the best dynamic performance of the DTC drive system. In this paper, a simple and low cost solution DTC scheme is suggested and implemented using a single chip and relatively low cost microcontroller of the family (SAB80C166). The experimental result indicates very good and fast dynamic performance of the suggested scheme. Where they indicates a torque and flux ripple reduction, and a less current distortion.

APPENDIX

Motor Parameters:

R_s = 1.2 ohm.
$L_s = L_d = L_q$ = 0.015 h.
j_m = 0.000176 Kg.m^2 .
B_m = 0.00038815 Nm/rad/sec.
λ_f = 0.2865 V/rad/sec.
P = 3 pair of pole.

Motor Ratings:

Line to Line Voltage = VLL_rms = 230 V.
Line to Line Current = ILL_rms = 6.4 A.
Vdc = 310.61 V.
Rated torque = Load_Torqe = 3.2 Nm.
Rated speed = speed_ref. = 419 rad/s. = 4000 rpm.
Rated frequency = f = 200 Hz, six poles.
Rated power = Pout =1.34 Kw.

REFERENCES

[1] M. A. Rahman and G.R. Slemon, "The promising applications of NdBFe magnets in electrical Machines (invited)", IEEE Trans. On Magnetics, Vol. MAG-21, no.5, 1985,pp.1712-1716.

[2] Saad Muftah Zeid, " An analysis of permanent magnet synchronous motor drive", M.Sc., Memorial University of Newfoundland, Canada, December 1998.

[3] A. R. Wheeler, "Comparison of electrical variable speed drives", Inti. Conf. on Power Electronics and Variable Speed Drives, lEE conf: Publication, no.234, London, 1984, pp. 175-179.

[4] Ah. A. Mahfouz , G. M. Sarhan , A. A. Nafeh , "Direct torque control of induction motor using intelligent controller" IEEE , MEPCON , pp.345-349, December 16-18, 2003.

[5] Ramin Monajemy" Control strategies and parameter compensation for permanent magnet synchronous motor drives", Ph.D., the Faculty of the Virginia Polytechnic Institute and State University, October 12, 2000.

[6] R. S. Colby , D. W. Novotny, " An efficiency-optimizing permanent-magnet synchronous motor drive" IEEE Trans. Ind. Applicat., vol. 24, no. 3, pp.462-469, May/June , 1988.

[7] Tian-hua Liu , Chung Young and Chang-huan Liu, " Microprocessor-based controller design and simulation for a permanent magnet synchronous motor drive" IEEE Trans. Ind. Electro. , vol. 35 , no. 4 , pp.516-523 , November , 1988.

[8] PRAG. PILLAY , and RAMU KRISHNAN , "Modeling, simulation and analysis of permanent-magnet motor drives, Part I: The Permanent-Magnet Synchronous Motor Drive" IEEE Trans. Ind. Applicat., vol.25, no.2, pp.265-273, March/April. 1989.

[9] Se-Kyo Chung, Hyun-Soo Kim, Chang-Gyun Kim, and Myung-Joong Youn, "A new instantaneous torque control of PM synchronous motor for high-performance direct-drive applications" IEEE Trans. Pow. Electron., vol. 13, no. 3, pp.388-400, May , 1998.

[10] Hans-Peter Nee, Louis Lefevre , Peter Thelin , and Juliette Soulard , "Determination of d and q reactances of permanent-magnet synchronous motors without measurements of the rotor position" IEEE Trans. Ind. Applicat. , vol. 36 , no.5, pp.1330-1335, September/October , 2000.

[11] P. C. Krause, "Analysis of electric machinery", McGraw Hill, 1986.

[12] Enrique L. Carrillo Arroyo, "Modeling and simulation of permanent magnet synchronous motor drive system", M.Sc., university of puerto rico , mayagüez campus, 2006.

[13] P. C. Krause, "Electromechanical motion devices", McGraw Hill, 1989.

[14] F. A. M. Osman, "Field oriented controller for brushless synchronous motor", M.Sc., Benha University, 2003.

[15] Rached Dhaouadi,Ned Mohan and Lars Norum ,"Design and implementation of an extended kalman filter for the State estimation of a permanent magnet synchronous motor" IEEE Trans. Power Electron., Vol. 6, no.3, pp.491-497, July,1991.

[16] A. A. A. Nafeh, "Direct torque control of induction motor using intelligent controller", Ph. D., Cairo University ,Giza , Egypt ,2004.

[17] Florent Morel, Xuefang Lin-Shi, Jean-Marie R´etif, Bruno Allard," A predictive current control applied to a permanent magnet synchronous machine, comparison with a classical direct torque control" Electric Power Systems Research, Vol.78, no.8, pp.1437-1447, August 2008.

[18] An. S. Salib, "Direct torque control of single-phase induction motor drives", M.Sc., Cairo University ,Giza , Egypt ,2004.

[19]http://mech2006.vtk.be/downloads_2eIr/Actuatoren/DTC .pdf ,2006 " Direct torque control versus field oriented control "

[20] Pawel Z. Grabowski, M. P. Kazmierkowski, B. K. Bose, andFrede Blaabjerg," A simple direct-torque neuro-fuzzy control of PWM-inverter-fed induction motor drive", IEEE Trans. on Ind. Elec., Vol. 47, No. 4, pp. 863-870, Aug. 2000.

[21] Ahmed A. Mahfouz, Gamal M. Sarhan, and Abdel-Nasser A. Nafeh, "Direct torque control of induction motor using intelligent controller", Proc. of IEEE MEPCON'03, Egypt, Vol. 1, Dec. 2003, pp. 345-349.

[22] I. Takahachi and T. Noguchi, "A new quick response and high efficiency control strategy of an induction machine", IEEE Trans. on Ind. Applications, Vol.1A-22, pp. 820-827, Sept./Oct. 1986.
[23] Y. A. Atia, "Enhanced efficiency pumping system operating with photovoltaic source", Ph.D. Thesis, Cairo University, 2000.
[24] D. Casadei, G. Grandi, G. Serra, and A. Tani, "Effects of flux and torque hysteresis band amplitude in direct torque control of induction machines", Proc. of IEEE IECON'94, Bolongna, Italy, Sept. 1994, pp. 299-304.
[25] E. Galvan, et al, " A family of switching control strategies for the reduction of torque ripple on the direct torque and flux control for induction motors", Proc. of IEEE IECON'01, 2001, pp.1274-1297.
[26] N.R.N. Idris and A.H.M. Yatim "Reduced torque ripple and constant torque switching frequency strategy for direct torque control of induction motor", Proc. of IEEE, APEC'OO, 2000, pp. 154-161.
[27] Kazmierkowski, M.P., "Control strategies for PWM rectifier/inverter-fed induction motors", Proc. of the IEEE - International Symposium on Industrial Electronic. (ISIE), Vol. 1,2000, pp. TUI5 -TU23.
[28] D. Casadei, et al, "Switching strategies in direct torque control of induction machines", Proc.of ICEM'94, Paris, pp. 204-209, 5-8 Sept., 1994.
[29] G. Buja, et al, "DTC based strategies for induction motor drives", Proc., of IEEE -IECON'97, pp. 1506-1516, 1997.
[30] A. A. A. Nafeh, "Microcontroller inverter fed three phase induction motor", Benha University, 2001.
[31] Chee-Mun Ong, "Dynamic Simulation of Electric Machinery Using Matlab/Simulink" Prentice-Hall PTR, New Jersey, 1998.
[32] The Math works Inc., "MATLAB User's Guide", Feb. 1993.
[33] P. Vas, "Sensorless vector and direct torque control" OXFORD, U.K. Oxford Univ. Press,1998.

Authors

Abdelnasser Nafeh was born in Egypt in 1971. He received

his B.Sc. and M.Sc. Degrees from Benha High Institute of Technology (BHIT), Benha University, Egypt, in 1995 and 2001, respectively. He received his Ph.D. from Cairo University, Egypt, in 2005. He joined the Department of Electrical Engineering, at BHIT, Benha University, Egypt, in 1997, and is currently an assistant Professor at BHIT. From 2007 to 2008 he is a postdoctoral fellowship at University of Waterloo, Ontario, Canada. His research interests are in the areas of Power Electronics, Electrical Machines, Electrical Drives, Control, Fuzzy logic control, and multilevel inverters.

Mohamed Shalan was born in Egypt in 1980. He received

his B.Sc. and M.Sc. Degrees from Benha High Institute of Technology (BHIT), Benha University, Egypt, in 2002 and 2009, respectively. He joined the Department of Electrical Engineering, at BHIT, Benha University, Egypt, in 2003, and is currently an assistant lecturer at BHIT. His research interests are in the areas of Power Electronics, Electrical Machines, Electrical Drives, Control, renewable energy.